Atmos. Chem. Phys. Discuss., 7, 1823–1847, 2007
www.atmos-chem-phys-discuss.net/7/1823/2007/

Atmospheric Chemistry and Physics Discussions

Enhanced tropospheric BrO concentrations over the Antarctic sea ice belt in mid winter observed from MAX-DOAS observations on board the research vessel Polarstern

T. Wagner[1], **O. Ibrahim**[2], **R. Sinreich**[2], **U. Frieß**[2], **and U. Platt**[2]

[1]Max-Planck-Institute for Chemistry, Mainz, Germany
[2]Institut für Umweltphysik, University of Heidelberg, Heidelberg, Germany

Received: 8 January 2007 – Accepted: 30 January 2007 – Published: 5 February 2007

Correspondence to: T. Wagner (thomas.wagner@iup.uni-heidelberg.de)

Abstract

We present Multi AXis-Differential Optical Absorption Spectroscopy (MAX-DOAS) observations of tropospheric BrO carried out on board the German research vessel Polarstern during the Antarctic winter 2006. Polarstern entered the area of first year sea ice around Antarctica on 24 June 2006 and stayed within this area until 15 August 2006. For the period when the ship cruised inside the first year sea ice belt, enhanced BrO concentrations were almost continuously observed. One interesting exception appeared on 7 July 2006, when the sun elevation angle was < about –2.8° indicating that for low insulation the photolysis of Br_2 and/or HOBr is too slow to provide sufficient amounts of Br radicals. Before and after the period inside the first year sea ice belt, typically low BrO concentrations were observed. Our observations indicate that enhanced BrO concentrations around Antarctica exist about one month earlier than observed by satellite instruments. The small BrO concentrations over the open oceans indicate a short atmospheric lifetime of activated bromine without contact to areas of first year sea ice. From detailed radiative transfer simulations we find that MAX-DOAS observations are about one order of magnitude more sensitive to near-surface BrO than satellite observations. In contrast to satellite observations the MAX-DOAS sensitivity hardly decreases for large solar zenith angles and is almost independent from the ground albedo. Thus this technique is very well suited for observations in polar regions close to the solar terminator. Furthermore, combination of both techniques could yield additional information on the vertical distribution of BrO in the lower troposphere.

1 Introduction

During the 1980's it was discovered that in the polar spring's troposphere the ozone concentrations occasionally dropped below the detection limit (Bottenheim et al., 1986; Oltmans and Komhyr, 1986; Solberg et al., 1996). Typically, low ozone values were observed for periods of several hours to several days and the phenomenon was termed

ACPD

7, 1823–1847, 2007

'troposheric ozone hole'. Only a few years later, Barrie et al. (1988) discovered that enhanced concentrations of tropospheric bromine compounds are very likely the cause for the very efficient ozone destruction. Later on, it was shown by several groups that in particular enhanced BrO concentrations are present during such episodes of tropospheric ozone depletion (Hausmann and Platt, 1994; Platt and Lehrer, 1996; Kreher et al., 1997; Tuckermann et al., 1997; Hönninger and Platt, 2002; Jacobi et al., 2006).

After the launch of the GOME instrument aboard the European research satellite ERS-2, it became possible for the first time to search the whole globe for enhanced tropospheric BrO concentrations and it was found that enhanced boundary layer BrO concentrations were indeed present over large areas in both polar regions during spring (Wagner and Platt, 1998; Richter et al., 1998; Wagner et al., 2001; Richter et al., 2002; Hollwedel et al., 2003). From these satellite observations also indications were found for a strong relation to the presence of first year sea ice (Wagner et al., 2001) and to areas covered by so called frost flowers (Kaleschke et al., 2004). Today, still uncertainties exist on the detailed release mechanisms of the reactive bromine compounds (see e.g. Sander et al., 2006, and references therein). In particular also the importance of different potential sources enriched in bromide is unclear: such sources could be provided e.g. by frost flowers, snow flakes fallen into enriched brine; aerosols enriched in bromide can be created by wind gusts on these surfaces, on the brine itself (Sander et al., 2006) or by other processes (Simpson et al., 2005).

Besides the satellite observations, only few ground based measurements have so far been carried out in regions where the enhanced boundary layer BrO concentrations actually appear, e.g. at Barrow, Alert, Hudson Bay in Canada, or Ny Alesund at Spitsbergen (Hausmann and Platt, 1994; Tuckermann et al., 1997; Lehrer,1999; Hönninger and Platt, 2002; Hönninger et al., 2004; Simpson et al., 2005). Especially in Antarctica and/or within areas of first year sea ice such observations are sparse (e.g. Kreher et al., 1997; Frieß et al., 2004). Thus, and because of several limitations of the satellite observations, still many open questions, not only on the details of the related chemistry (see e.g. Sander et al., 2006) but also on the characteristic circumstances necessary

for the occurrence of enhanced BrO concentrations remain.

In particular, it is unclear when and under which conditions the enhanced boundary layer BrO concentrations first appear in polar spring. From satellite observations the first events are typically found in mid January (Arctic) and at the end of July (Antarctica) (Wagner et al., 2001). However, satellite observations of boundary layer BrO are only possible if the sun is clearly above the horizon. For measurements at solar zenith angles (SZA) larger than about 87°, the sensitivity towards boundary layer BrO strongly decreases while that for stratospheric BrO strongly increases (Wagner et al., 2001) (see also Sect. 3.2). This dependence on the solar elevation prevents the unambiguous detection of enhanced boundary layer BrO concentrations for the period directly after the end of the polar night.

Another important question concerns the spatial extension of the clouds of enhanced BrO concentrations. The areas of enhanced BrO concentrations can have dimensions of up to thousands of kilometres which can well be observed by satellite instruments. However, the ground pixel size of satellite observations is still too large to resolve gradients on scales of only kilometres. Thus possible clouds of enhanced BrO concentrations with smaller dimensions are difficult to be observed. Similarly, also small air masses without enhanced BrO concentrations in regions with otherwise enhanced BrO might be overlooked. Another limitation of the satellite observations is that in many cases enhanced BrO concentrations might be shielded by clouds. Thus, in some situations, when no enhanced BrO concentrations are observed, it remains unclear if actually no enhanced BrO concentrations exist or if they are simply shielded by clouds.

Finally, it is not clear, how far the clouds of enhanced BrO concentrations can be transported away from their source regions. Strongly enhanced BrO concentrations have so far only been observed over areas of first year sea ice or very close to them (e.g. Wagner et al., 2001; Frieß et al., 2004; Kaleschke et al., 2004). In particular, it is unclear how far clouds of enhanced BrO concentrations might be transported over the open ocean. From satellite observations over the open ocean typically no enhanced BrO concentrations are detected (with very few exceptions). Because of the low sur-

ACPD
7, 1823–1847, 2007

face albedo of the ocean surface the sensitivity of the satellite observations is strongly reduced compared to observations over snow and ice (see Sect. 3.2). Thus, especially for observations over oceanic regions close to the edge of the sea ice it remains unclear if actually no enhanced BrO concentrations exist or if they are just not "seen" by the satellite instrument.

Here we present Multi AXis-Differential Optical Absorption Spectroscopy (MAX-DOAS) observations made on the research vessel Polarstern during austral winter 2006 (details on the cruise can be found at the Polarstern web-page of the Alfred-Wegener Institute: http://www.awi-bremerhaven.de/Polar/polarstern.html). From these observations new information on the above mentioned open questions could be derived. The main advantage of these measurements is that they were performed on board of an ice breaker, which directly crossed the areas of first year sea ice. MAX-DOAS observations are performed in various slant viewing directions, which make them especially sensitive to tropospheric trace gases (Leser et al., 2003; Van Roozendael et al., 2003; Wittrock et al., 2003; Hönninger et al., 2004; Wagner et al., 2004; Sinreich et al., 2005; Heckel et al., 2005; Frieß et al., 2006; Wagner et al., 2006). One specific advantage of MAX-DOAS observations is that they remain sensitive towards boundary layer BrO concentrations even for large SZA (see Sect. 3.2), thus enabling measurements directly after the end of the polar night. Finally, the sensitivity of MAX-DOAS observations is very similar over areas of high albedo (snow and ice) and low albedo (ocean). Thus possible high boundary layer BrO concentrations over the open ocean can be unambiguously detected.

2 Ship cruise and instrumental set-up

The MAX-DOAS instrument was installed on board the research vessel Polarstern in October 2005 and since then continuously performed automatic measurements during the entire cruise (see also cruise information at: http://www.awi-bremerhaven.de/Polar/polarstern.html). In austral winter 2006, Polarstern penetrated into the first year sea ice

ACPD
7, 1823–1847, 2007

area which surrounds the Antarctic continent; the first contact was on 24 June 2006 at 59.5° S, 5.0° E. On its way back, Polarstern left the sea ice belt on 15 August 2006 at about 55.5° S, 3° E. The sea ice in the area which Polarstern crossed was almost exclusively first year sea ice, containing cracks, polynyas and areas with Nilas and young ice (L. Kaleschke, personal communication).

During the whole path within the sea ice belt, the solar zenith angle was rather large. At the beginning, the daily minimum values were around 80°; from 3 July to 7 July they stayed >90°; after 14 August they reached values <70°. Even on the days with large SZA, successful MAX-DOAS measurements of enhanced tropospheric BrO were possible (except for five days at the beginning of July).

The MAX-DOAS instrument consists of an indoor and an outdoor set-up. Both are connected via electric cables and glass fibres. The telescope is mounted in a small heated box, which is moved by a stepper motor to allow elevation angles (α) between 0° (pointing to the horizon) and 90° (pointing to the zenith); the sequence of elevation angles is 1°, 3°, 6°, 10°, 30°, 90°.

The light is fed into an Ocean Optics USB 2000 spectrograph that disperses the light with a grating and maps it onto a one dimensional CCD array with 2048 elements. The wavelength range reaches from 290 nm to 430 nm, thus enabling the analysis of various trace gases including e.g. O_3, NO_2, BrO, OClO, HCHO, and SO_2. The spectral resolution is about 0.9 nm (full width at half maximum).

The spectrometer is mounted into a modified hermetic Dewar vessel. In order to avoid ambient air from penetrating into the protective vessel it had been evacuated and filled up with gaseous Argon up to 1.2 bar prior to the expedition. Stable measurement conditions and low detector noise could be achieved by cooling the spectrograph down to approx. 0°C by a two-stage Peltier cooling unit. Spectra are taken about every 2 minutes between sunrise and sunset. During the night (for SZA >97°) automatic measurements of offset and dark current are taken. The correct time (UTC) and position of the ship is provided from the on board computer system.

ACPD
7, 1823–1847, 2007

3 Data analysis

3.1 Spectral retrieval

The measured spectra are analysed using the DOAS method (Platt, 1994). To the (logarithm of the) measured spectrum several trace gas cross sections as well as a Ring spectrum (Grainger and Ring, 1962; Bussemer, 1993), a Fraunhofer reference spectrum and a polynomial of low degree are fitted by means of a least squares fitting routine (Gomer et al., 1993; Stutz and Platt, 1996). To extract the tropospheric absorptions from the measured spectra (taken at low elevation angles), the Fraunhofer spectrum was always taken from the directly preceding zenith observation. For the BrO analysis, the wavelength range 335.3–358.9 nm was used and the cross sections of ozone (223 and 243 K, Bogumil et al., 2003), NO_2 (220 K, Vandaele et al., 1997), BrO (Wilmouth et al., 1999), and the oxygen dimer O_4 (Greenblatt et al., 1990) were included. The Ring spectrum was calculated from a measured spectrum (Bussemer et al., 1993). For the O_4 analysis the wavelength range 345.0–364.5 nm was used and the cross sections of ozone (223 K), NO_2, BrO, and O_4 were included. The wavelength calibration was performed by fitting the measured spectra to a high resolution solar spectrum (Kurucz et al., 1984). From the spectral analysis the so called slant column density (SCD) is retrieved, which is the integrated trace gas concentration along the light path through the atmosphere.

Because the Fraunhofer spectrum also contains atmospheric absorption structures of the atmospheric trace gases, the result of the DOAS analysis represents the difference of the SCDs of the measured spectrum and of the Fraunhofer spectrum. In the following we will refer to them as differential slant column densities ($\Delta SCD = SCD_{meas} - SCD_{ref}$). Since the Fraunhofer spectrum was measured in zenith direction, the respective tropospheric absorptions are typically very weak compared to those measured at low elevation angles. Thus the measured ΔSCD is roughly proportional to the tropospheric concentration. For the detailed interpretation of the retrieved ΔSCD radiative transfer modelling has to be applied.

ACPD
7, 1823–1847, 2007

EGU

3.2 Radiative transfer modelling

In this section we present results of radiative transfer modeling using our Monte Carlo model "TRACY-2" (Deutschmann et al., 2006; Wagner et al., 2006), which takes into account multiple scattering, and full sphericity. From our model results we can particularly estimate the sensitivity of the MAX-DOAS observations for boundary layer BrO under different measurement conditions. Usually the results of radiative transfer modelling are expressed as air mass factors (AMF), which represent the ratio between the slant column density (SCD) and the vertical column density (VCD) (Noxon et al., 1979; Solomon et al., 1987; Marquard et al., 2000).

$$\mathrm{AMF} = \mathrm{SCD}/\mathrm{VCD} \tag{1}$$

The AMF can in particular be seen as an indicator for the sensitivity of the observation. The AMF of MAX-DOAS observations of tropospheric species can reach especially large values (AMF>30). Since the results of the MAX-DOAS observations are expressed as ΔSCD, we also calculate so called 'differential AMF' (ΔAMF(α) = AMF(α) – AMF(90°)) by subtracting the modelled AMF for the zenith direction (elevation angle α = 90°) from the modelled AMFs for the low elevation angles (α). The VCDs can then be derived by dividing the measured ΔSCD by the appropriate ΔAMF.

$$\mathrm{VCD} = \frac{\Delta\mathrm{SCD}}{\Delta\mathrm{AMF}} = \frac{\mathrm{SCD}\,(\alpha) - \mathrm{SCD}\,(90^\circ)}{\mathrm{AMF}\,(\alpha) - \mathrm{AMF}\,(90^\circ)} \tag{2}$$

It should be noted that the AMF for the zenith direction is usually close to unity; thus especially for the large AMFs at low elevation angles the ΔAMF can be approximated by the AMF.

The sensitivity (the ΔAMF) of MAX-DOAS observation strongly depends on the atmospheric visibility (Wagner et al., 2004; Heckel et al., 2005; Frieß et al., 2006). In the presence of aerosols or clouds, the sensitivity can be strongly reduced. Especially in the case of fog, the atmospheric absorption paths for all viewing directions (including

ACPD
7, 1823–1847, 2007

EGU

the zenith direction) can become very similar; consequently for such cases the ΔSCDs and ΔAMFs become zero.

To estimate the atmospheric visibility we investigated the simultaneously observed absorptions of O_4. Since the oxygen content of the atmosphere varies only slightly (due to temperature and pressure variations), the variations of the observed O_4 ΔSCD can be used as an indicator for variations of the atmospheric radiative transfer. Especially situations with a poor visibility, e.g. due to fog, can be identified by low O_4 ΔSCDs.

In the following examples we investigate the sensitivity of MAX-DOAS observations to surface near BrO concentrations and the O_4 absorption. Our particular interest is on the dependence of the sensitivity on the atmospheric visibility and the surface albedo.

In our first modelling case study we simulate the atmospheric radiative transfer at 350 nm for the different elevation angles (1°, 3°, 6°, 10°, 30°, 90°) for various atmospheric aerosol loads. We calculate ΔAMFs for three different height profiles assuming a surface albedo of 80%: the first profile (BrO-1) describes constant BrO concentrations between the surface and 200 m altitude. The second profile (BrO-2) describes constant BrO concentrations between the surface and 1000 m altitude (very similar results are obtained if constant mixing ratios are assumed). The third profile (O_4) has the relative shape of the atmospheric O_4 profile (proportional to the quadratic O_2 concentration, see e.g. Greenblatt et al., 1990). For clear sky (Fig. 1a) the ΔAMFs strongly increase with decreasing elevation angle. Especially for the surface-near profile (BrO-1) the ΔAMF can become very high (up to about 40) indicating the high sensitivity of MAX-DOAS observations; for the other profiles the ΔAMF are systematically smaller. This difference is caused by the fact that most photons are scattered into the instrument from rather low altitudes. For trace gases below this altitude the absorption paths are mainly slant and therefore long. For trace gases above this altitude, the absorption paths are much smaller. With increasing aerosol optical density, the extension of the slant absorption paths become shorter. Correspondingly, the ΔAMF become smaller and finally close to zero for all elevation angles (Figs. 1b, c).

ACPD
7, 1823–1847, 2007

We also investigated one very interesting situation: the case that the aerosol (or fog) layer does not reach down to the surface. Figure 1d shows ΔAMFs for an aerosol layer between 200 and 1200 m altitude. While the O_4ΔAMFs are very small, those for both BrO profiles are still substantially larger than zero. Especially for the assumed BrO layer between the surface and 200 m (BrO-1), the BrO ΔAMFs are similar to the clear sky case (Fig. 1a). These results are important for the understanding of measurements, where enhanced BrO ΔSCDs are accompanied by very small O_4ΔSCDs (see Sect. 4).

It is interesting to compare the ΔAMFs for MAX-DOAS observations with the AMFs for satellite viewing geometry (Fig. 1e). For satellite observations, usually a Fraunhofer reference spectrum without tropospheric BrO absorptions (e.g. an extraterrestrial solar spectrum) is used; thus the result of the spectral analysis represents the total atmospheric slant column density and the appropriate results of radiative transfer modelling are AMF (instead of ΔAMF). For most cases, the ΔAMFs for MAX-DOAS observations are much larger (10–40) than the satellite AMF (<1–3) indicating the high sensitivity of the MAX-DOAS measurements. Another interesting finding is that the satellite AMFs for O_4 are almost independent of the aerosol optical density, and also the AMFs for both BrO profiles stay still clearly above zero (although they decrease substantially with increasing optical density). This means that over bright surfaces even in the case of fog or clouds, satellite observations are still sensitive to trace gases close to the ground, indicating that a significant fraction of the photons which have penetrated the aerosol or cloud layer can still reach the satellite instrument.

In a second study, we investigated ΔAMFs for MAX-DOAS observations for various SZA and surface albedos. For these calculations we only considered the elevation angle of 1°, since it exhibits the highest sensitivity for trace gases located directly above the surface. We also did not include scattering by aerosols and clouds; thus our results represent only upper limits of the respective ΔAMFs (Wagner et al., 2004). However, such upper limits are important to estimate the corresponding lower limits for the tropospheric BrO VCD (and the respective boundary layer BrO concentrations) (see Eq. 2).

ACPD
7, 1823–1847, 2007

The ΔAMFs for the three different trace gas profiles are shown in Fig. 2a. The ΔAMFs only slightly depend on the SZA and the surface albedo, making MAX-DOAS observations very sensitive to tropospheric trace gases even at high SZA and low albedo. This advantage becomes especially obvious when the ΔAMFs are compared to the AMFs for satellite observations (Fig. 2b). In contrast to the MAX-DOAS observations, the AMFs for satellite viewing geometry strongly decrease with increasing SZA and decreasing albedo.

4 Results

In Fig. 3 typical results for selected days of the ship cruise are presented. For the detailed interpretation of the observed BrO ΔSCDs also the simultaneously observed O_4ΔSCDs are presented. Furthermore, observations of the horizontal atmospheric visibility and the ceiling height derived from the on board monitoring system of the ship (available via: http://www.awi-bremerhaven.de/MET/Polarstern/poldatquery.html) are shown. For cloud ceilings above about 1km, the O_4 absorption is mainly limited by the atmospheric visibility (for an elevation angle of 1° the light path between the telescope and the cloud base is 1 km/sin(1°) ≈57 km).

In Fig. 3a results for a day before Polarstern reached the sea ice area (18 June 2006) are presented. The O_4ΔSCDs are high and show a clearly repeating cycle corresponding to the sequence of telescope elevation angles. Such a temporal pattern is obtained if the O_4 absorptions at the different elevation angles are systematically different, which is a strong indication for a high atmospheric visibility (in good agreement with the measurements of the on board instrumentation). For the clear sky period of this day the maximum O_4ΔSCDs are about 6.5×10^{43} molec^2/cm^5 (e.g. between about 09:00 and 12:00) which is in good agreement with the model results for a clear day (for an O_4 VCD of about 1.3×10^{43} molec^2/cm^5 they correspond to a ΔAMF of about 5). Also the onboard measurements of the ceiling height show an almost clear sky for this period. In contrast to the O_4ΔSCDs, on this day the BrO ΔSCDs show no enhanced values

ACPD
7, 1823–1847, 2007

indicating that no enhanced boundary layer BrO concentration was present. All other results shown in Fig. 3 (b to f) are derived on days when the ship was inside the area of first year sea ice. On these days typically high BrO ΔSCDs are observed. There are two interesting exceptions: on 08.08. (Fig. 3d) the BrO ΔSCDs during the first half of the day are close to zero. Since the O_4 ΔSCDs of this day are high (also the visibility is relatively high), this indicates that the surface near BrO concentrations are actually very low. It should be noted that similar results of very low BrO concentrations were only very rarely found during the whole period the ship was inside the area of first year sea ice (at the end of 24.07.; at the end of 03.08.; in the afternoon of 07.08.; in the main part of the morning of 08.08.; in the morning and evening of 14.08.).

Also in the first half of 10.08. (Fig. 3f) low BrO ΔSCDs are measured. However, in this case they do very probably not indicate low BrO concentrations, but rather low atmospheric visibility (as also indicated by the on board measurements and the low O_4ΔSCDs).

Another interesting result is that on several days high BrO ΔSCDs, but rather low O_4ΔSCDs are observed (e.g. 25.07. and 09.08., see Figs. 3b, e). Especially on 09.08. the cloud ceiling (between about 100 and 200 m) and the visibility were very low. The enhanced BrO ΔSCDs indicate that high BrO concentrations have been mainly present below the cloud.

In Figs. 4 and 5 the daily maximum BrO ΔSCDs are presented from 17 June until 21 August 2006. In addition, also the latitude of the ship and that of the ice edge, the daily maximum global radiation (from the on board instrumentation), the daily maximum sun elevation angle as well as the temperatures of the air and the water are shown. The period when the ship was inside the sea ice can be clearly determined from the latitude plot and the time when the water temperatures were below zero. Before and after the ship reaches the area of first year sea ice, only small BrO ΔSCDs are observed. Enhanced BrO ΔSCDs are almost entirely found during the period when the ship was within the area of first year sea ice. One interesting exception appeared on 7 July 2006. On this day the sun elevation was very low (<2.8°) indicating that the photolysis of BrO

ACPD
7, 1823–1847, 2007

EGU

and/or HOBr might have been too slow to provide sufficient amounts of Br radicals. On the previous day (6 July 2006) the sun elevation reached a maximum value of –1.5° and still enhanced BrO ΔSCDs were observed. It should, however, be noted that for measurements with sun elevation <0° the measurement error can become very large and the respective BrO ΔSCDs might only be seen as an indicator for the true BrO ΔSCDs. Days with such large errors include the 6, 7, 11, and 13 July, when the optical density of the residual was up to 3%. For several other days during low sun elevation, the residual was even larger and no meaningful retrievals were possible at all.

Our measurements indicate that enhanced boundary layer BrO concentrations almost continuously exist over the sea ice for the whole period the ship is present there. After the ship left the area of first year sea ice, again only low BrO ΔSCDs were found indicating a short lifetime of the activated bromine compounds. Another important finding is that events of enhanced BrO concentrations are observed by the MAX-DOAS observations about one month earlier than from satellite observations (Wagner et al., 2001).

Using the modelled ΔAMF we can convert the measured ΔSCDs into BrO concentrations and BrO mixing ratios. We apply this conversion for the telescope elevation of 1° and we consider again the two BrO profiles described in Sect. 3.2. We also assume clear sky conditions, thus our conversion represents a lower limit for the true BrO concentrations.

For the BrO layer between the surface and 200 m the ΔAMF is about 39. Thus the measured ΔSCDs have to be divided by a factor of $39*2*10^4$ cm = $7.8*10^5$ cm. For a BrO layer between the surface and 1000m the ΔAMF is about 15. Thus the measured ΔSCDs have to be divided by a factor of $15*1*10^5$ cm = $1.5*10^6$ cm. Although both profile heights differ by a factor of 5, the conversion factors differ by only about a factor of two. This indicates that the conversion into BrO concentrations is rather insensitive on the assumptions of the layer height.

The retrieved BrO concentrations can be further converted into mixing ratios. Assuming e.g. a measured BrO ΔSCD of 10^{15} molec/cm^2 (about the maximum value during

ACPD
7, 1823–1847, 2007

EGU

the cruise) results in mixing ratios between 26 ppt and 51 ppt for the profile between the surface and 1000 m or between the surface and 200 m, respectively. These values are in good agreement with other measurements (e.g. Tuckermann et al., 1997; Wagner and Platt, 1998; Hönninger and Platt, 2002; Hönninger et al., 2004)

5 Conclusions

We performed MAX-DOAS observations of tropospheric BrO on board the German research vessel Polarstern during the Antarctic winter 2006. Polarstern entered the area of first year sea ice around Antarctica on 24 June 2006 and stayed within this area until 15 August 2006. For the period inside the area of first year sea ice, enhanced BrO concentrations were almost continuously observed. One interesting exception appeared on 7 July 2006, when the sun elevation angle was < about –2° indicating that for these low elevation angles the photolysis of Br_2 and/or HOBr is too slow to provide sufficient amounts of Br radicals. Our MAX-DOAS observations found enhanced BrO concentrations about one month earlier than analysed from satellite observations (Wagner et al., 2001). Before and after the period inside the first year sea ice, typically low BrO concentrations are observed. The small BrO concentrations over the open ocean indicate a short atmospheric lifetime of activated bromine compounds after the contact to areas of first year sea ice.

Even for days with very low cloud ceiling (between 100 and 200 m), large BrO ΔSCDs were observed (in contrast to those of O_4) indicating that the enhanced BrO concentrations are present close to the ground. From detailed radiative transfer simulations we find that MAX-DOAS observations are about one order of magnitude more sensitive compared to satellite observations. In contrast to satellite observations their sensitivity does hardly decrease for large solar zenith angles and low albedo. Thus they are very well suited for observations in polar regions close to the terminator. Our radiative transfer simulations also indicate that the inferred surface near BrO concentrations are not very sensitive to the assumed altitude range. The retrieved BrO concentrations are

ACPD
7, 1823–1847, 2007

EGU

in the order of several ten ppts in agreement with other observations and model results (e.g. Tuckermann et al., 1997; Wagner and Platt, 1998; Hönninger and Platt, 2002; Hönninger et al., 2004; Sander et al., 2006).

Acknowledgements. We like to thank the Alfred Wegner Institute in Bremerhaven for providing the opportunity to perform the MAX-DOAS observation on board of the research vessel Polarstern. Very special thanks are expressed to the crew, and in particular P. Gerschow, S. El Dine El Naggar, M. Rutgers van der Loeff and C. Schlosser for their great support. The onboard data are from the web-interface (http://www.awi-bremerhaven.de/MET/Polarstern/poldatquery.html) managed by G. König-Langlo, and the sea ice data are from the web page of the sea ice group of the National Centers for Environmental Prediction (NCEP) and the Marine Modelling and Analysis Branch (MMAB) (http://polar.ncep.noaa.gov/seaice/). We want to thank R. von Glasow, L. Kaleschke, and R. Sander for very stimulating discussions.

References

Barrie L. A., Bottenheim, J. W., Schnell, R. C., Crutzen, P. J., and Rasmussen, R. A.: Ozone destruction and photochemical reactions at polar sunrise in the lower Arctic atmosphere, Nature, 334, 138–141, 1988.

Bogumil, K., Orphal, J., Homann, T., Voigt, S., Spietz, P., Fleischmann, O. C., Vogel, A., Hartmann, M., Bovensmann, H., Frerik, J., and Burrows, J. P.: Measurements of Molecular Absorption Spectra with the SCIAMACHY Pre-Flight Model: Instrument Characterization and Reference Data for Atmospheric Remote-Sensing in the 230–2380 nm Region, J. Photochem. Photobiol. A., 157, 167–184, 2003.

Bottenheim, J. W., Gallant, A. C., and Brice, K. A.: Measurements of NO_y species and O_3 at 82° N latitude, Geophys. Res. Lett., 13, 113–116, 1986.

Burrows, J. P., Weber, M., Buchwitz, M., Rozanov, V., Ladstätter-Weißenmayer, A., Richter, A., DeBeek, R., Hoogen, R., Bramstedt, K., Eichmann, K.-U., Eisinger, M., and Perner, D.: The Global Ozone Monitoring Experiment (GOME): Mission Concept and First Scientific Results, J. Atmos. Sci., 56, 151–175, 1999.

Bussemer, M.: Der Ring-Effekt: Ursachen und Einfluß auf die Messung stratospärischer Spurenstoffe, Diploma Thesis, University of Heidelberg, 1993.

Deutschmann, T. and Wagner, T.: TRACY-II Users manual, University of Heidelberg, 2006.
ESA Publication Division (SP-1182), GOME, Global Ozone Monitoring Experiment, users manual, edited by: Bednarz, F., European Space Research and Technology Centre (ESTEC), Frascati, Italy, 1995.
Frieß, U., Hollwedel, J., Koenig-Langlo, G., Wagner, T., and Platt, U.: Dynamics and chemistry of tropospheric bromine explosion events in the Antarctic, J. Geophys. Res., 109, D06305, doi:10.1029/2003JD004133, 2004.
Frieß, U., Monks, P. S., Remedios, J. J., Rozanov, A., Sinreich, R., Wagner, T., and Platt, U.: MAX-DOAS O4 measurements: A new technique to derive information on atmospheric aerosols. (II) Modelling studies, J. Geophys. Res., 111, D14203, doi:10.1029/2005JD006618, 2006.
Gomer, T., Brauers, T., Heintz, F., Stutz, J., and Platt, U.: MFC user manual, version 1.98, Institut für Umweltphysik, University of Heidelberg, Germany, (http://ich313.ich.kfa-juelich.de/Mfc/mfc.htm), 1993.
Grainger, J. F. and Ring, J.: Anomalous Fraunhofer line profiles, Nature, 193, 762, 1962.
Greenblatt, G. D., Orlando, J. J., Burkholder, J. B., and Ravishankara, A. R.: Absorption measurements of oxygen between 330 and 1140 nm, J. Geophys. Res., 95, 18 577–18 582, 1990.
Hausmann, M. and Platt, U.: Spectroscopic measurement of bromine oxide and ozone in the high Arctic during Polar Sunrise Experiment 1992, J. Geophys. Res., 99, 25 399–25 414, 1994.
Heckel, A., Richter, A., Tarsu, T., Wittrock, F., Hak, C., Pundt, I., Junkermann, W., and Burrows, J. P.: MAX-DOAS measurements of formaldehyde in the Po-Valley, Atmos. Chem. Phys., 5, 909–918, 2005, http://www.atmos-chem-phys.net/5/909/2005/.
Hönninger, G. and Platt, U.: The Role of BrO and its Vertical Distribution during Surface Ozone Depletion at Alert, Atmos. Environ., 36, 2481–2489, 2002.
Hönninger, G., von Friedeburg, C., and Platt, U.: Multi Axis Differential Optical Absorption Spectroscopy (MAX-DOAS), Atmos. Chem. Phys., 4, 231–254, 2004, http://www.atmos-chem-phys.net/4/231/2004/.
Hollwedel, J., Wenig, M., Beirle, S., Kraus, S., Kühl, S., Wilms-Grabe, W., Platt, U., and Wagner, T.: Year-to-year variations of spring time polar tropospheric BrO as seen by GOME, Adv. Space Res., 804–808, 2004.

Jacobi, H.-W., Kaleschke, L., Richter, A., Rozanov, A., and Burrows, J. P.: Observation of a fast ozone loss in the marginal ice zone of the Arctic Ocean, J. Geophys. Res., 111, D15309, doi:10.1029/2005JD006715, 2006.

Kaleschke, L., Richter, A., Burrows, J. P., Afe, O., Heygster, G., Notholt, J., Rankin, A. M., Roscoe, H. K., Hollwedel, J., Wagner, T., and Jacobi, H.-W.: Frost flowers on sea ice as a source of sea salt and their influence on tropospheric halogen chemistry, Geophys. Res. Lett., 31, L16114, doi:10.1029/2004GL020655, 2004.

Kreher, K., Johnston, P. V., Wood, S. W., and Platt, U.: Ground-based measurements of tropospheric and stratospheric BrO at Arrival Heights (78° S), Antarctica, Geophys. Res. Lett., 24, 3021–3024 (1997).

Kurucz, R. L., Furenlid, I., Brault, J., and Testerman, L.: Solar flux atlas from 296 nm to 1300 nm, National Solar Observatory Atlas No. 1, 1984.

Lehrer, E.: Das polare troposphärische 'Ozonloch,' Ph.D. thesis, Univ. of Heidelberg, Heidelberg, Germany, 1999.

Leser, H., Hönninger, G., and Platt, U.: MAX-DOAS measurements of BrO and NO2 in the marine boundary layer, Geophys. Res. Lett., 30(10), doi:10.1029/2002GL015811, 2003.

Marquard, L. C., Wagner, T., and Platt, U.: Improved Air Mass Factor Concepts for Scattered Radiation Differential Optical Absorption Spectroscopy of Atmospheric Species, J. Geophys. Res., 105, 1315–1327, 2000.

Noxon, J. F., Whipple, E. C., and Hyde, R. S.: Stratospheric NO_2. 1. Observational method and behaviour at midlatitudes, J. Geophys. Res, 84, 5047–5076, 1979.

Oltmans, S. J. and Komhyr, W. D.: Surface ozone distributions and variations from 1973–1984 measurements at the NOAA geophysical monitoring for climatic change baseline observatories, J. Geophys. Res., 91, 5229–5236, 1986.

Platt, U. and Lehrer, E.: ARCTOC final report to EU, Brussels, 1996.

Richter, A., Wittrock, F., Eisinger, M., and Burrows, J. P.: GOME observations of tropospheric BrO in northern hemispheric spring and summer 1997, Geophys. Res. Lett., 25, 2683–2686, 1998.

Richter, A., Wittrock, F., Ladstätter-Weißenmayer, A., and Burrows, J. P.: GOME measurements of stratospheric and tropospheric BrO, Adv. Space Res., 29(11), 1667–1672, 2002.

Sander, R., Burrows, J., and Kaleschke, L.: Carbonate precipitation in brine the trigger for tropospheric ozone depletion events, Atmos. Chem. Phys., 6, 4653–4658, 2006, http://www.atmos-chem-phys.net/6/4653/2006/.

Simpson, W. R., Alvarez-Aviles, L., Douglas, T. A., Sturm, M., and Domine, F.: Halogens in the coastal snow pack near Barrow, Alaska: Evidence for active bromine air-snow chemistry during springtime, Geophys. Res. Lett., 32, doi:10.1029/2004GL021748, 2005.

Sinreich, R., Frieß, U., Wagner, T., and Platt, U.: Multi axis differential optical absorption spectroscopy (MAX-DOAS) of gas and aerosol distributions, Faraday Discuss., 130, 153, doi:10.1039/b419274, 2005.

Solberg, S., Schmidbauer, N., Semb, A., Stordal, F., and Øystein, H.: Boundary layer ozone depletion as seen in the Norwegian Arctic in spring, J. Atmos. Chem., 23, 301–332, 1996.

Solomon, S., Schmeltekopf, A. L., and Sanders, R. W.: On the interpretation of zenith sky absorption measurements, J. Geophys. Res., 92, 8311–8319, 1987.

Stutz, J. and Platt, U.: Numerical Analyses and Estimation of the Statistical Error of Differential Optical Absorption Spectroscopy Measurements with Least Square Methods, Appl. Opt., 35, 6041-6053, 1996.

Tuckermann, M., Ackermann, R., Gölz, C., Lorenzen-Schmidt, H., Senne, T., Stutz, J., Trost, B., Unold, W., and Platt, U.: DOAS-observation of halogen radical-catalysed Arctic boundary layer ozone destruction during the ARCTOC-campaigns 1995 and 1996 in Ny-Alesund, Spitsbergen, Tellus 49B, 533–555, 1997.

Vandaele, A. C., Hermans, C., Simon, P. C., Carleer, M., Colin, R., Fally, S., Mérienne, M.-F., Jenouvrier, A., and Coquart, B.: Measurements of the NO_2 Absorption Cross-section from 42 000 cm^{-1} to 10 000 cm^{-1} (238–1000 nm) at 220 K and 294 K, J. Quant. Spectrosc. Radiat. Transfer, 59, 171–184, 1997.

Van Roozendael, M., Fayt, C., Post, P., Hermans, C., and Lambert, J.-C.: Retrieval of BrO and NO_2 from UV-Visible Observations, in: Sounding the troposphere from space: a new era for atmospheric chemistry, Springer-Verlag, ISBN 3-540-40873-8, edited by: Borell, P., Burrows, J. P., Platt, U., 2003.

Wagner, T. and Platt, U.: Satellite mapping of enhanced BrO concentrations in the troposphere, Nature, 395, 486–490, 1998.

Wagner, T., Leue, C., Wenig, M., Pfeilsticker, K., and Platt, U.: Spatial and temporal distribution of enhanced boundary layer BrO concentrations measured by the GOME instrument aboard ERS-2, J. Geophys. Res., 106, 24 225–24 236, 2001.

Wagner, T., Dix, B., Friedeburg, C. v., Frieß, U., Sanghavi, S., Sinreich, R., and Platt, U.: MAX-DOAS O4 measurements – a new technique to derive information on atmospheric aerosols. (I) Principles and information content, J. Geophys. Res., 109, D22205,

doi:10.1029/2004JD004904, 2004.

Wagner, T., Burrows, J. P., Deutschmann, T., Dix, B., Hendrick, F., v.Friedeburg, C., Frieß, U., Heue, K.-P., Irie, H., Iwabuchi, H., Kanaya, Y., Keller, J., McLinden, C. A., Oetjen, H., Palazzi, E., Petritoli, A., Platt, U., Postylyakov, O., Pukite, J., Richter, A., van Roozendael, M., Rozanov, A., Rozanov, V., Sinreich, R., Sanghavi, S., and Wittrock, F.: Comparison of Box-Air-Mass-Factors and Radiances for Multiple-Axis Differential Optical Absorption Spectroscopy (MAX-DOAS) Geometries calculated from different UV/visible Radiative Transfer Models, Atmos. Chem. Phys. Discuss., 6, 9823–9876, 2006, http://www.atmos-chem-phys-discuss.net/6/9823/2006/.

Wittrock, F., Oetjen, H., Richter, A., Fietkau, S., Medeke, T., Rozanov, A., and Burrows, J. P.: MAX-DOAS measurements of atmospheric trace gases in Ny-Ålesund, Atmos. Chem. Phys., 4, 955–966, 2004, http://www.atmos-chem-phys.net/4/955/2004/.

Wilmouth, D. M., Hanisco, T. F., Donahue, N. M., and Anderson, J. G.: Fourier transfor ultraviolet spectroscopy of the $A^{2\Pi}_{3/2} \leftarrow X^{2\Pi}_{3/2}$ transition of BrO, J. Phys. Chem. A., 103, 8935–8945, 1999.

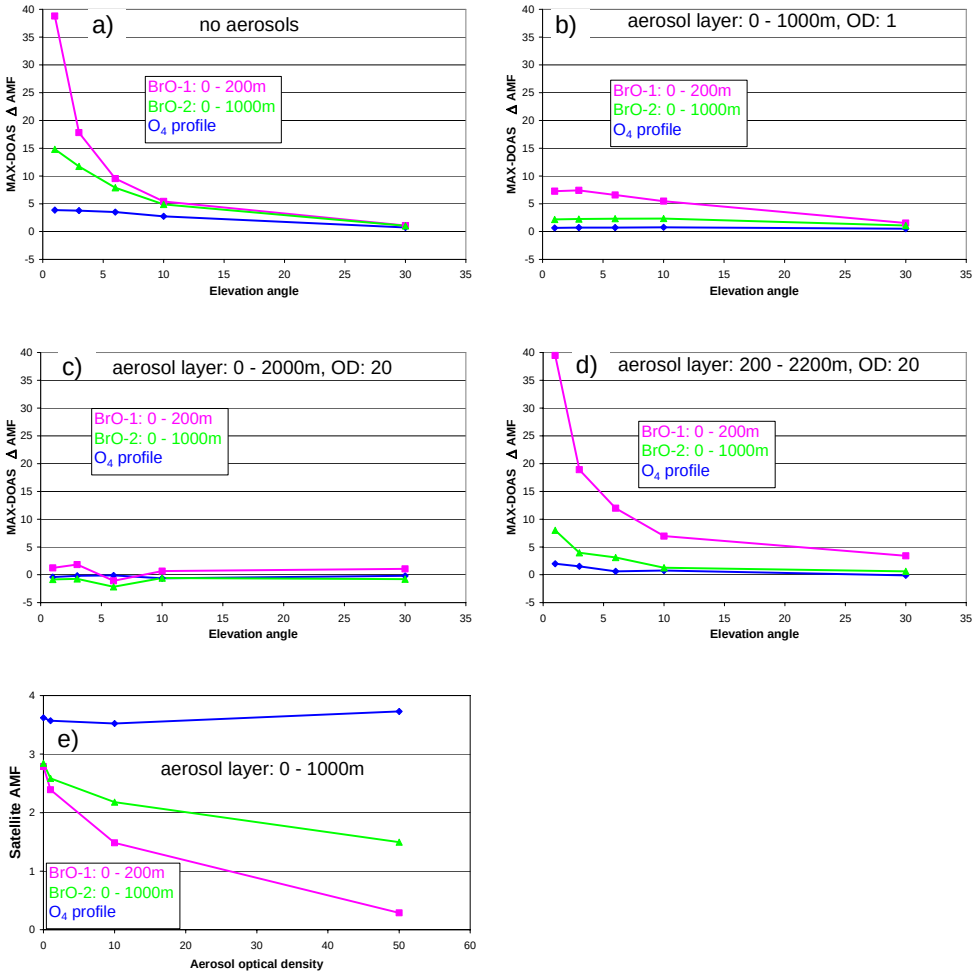

Fig. 1.

ACPD
7, 1823–1847, 2007

Fig. 1. Modelled sensitivity of MAX-DOAS observations (**a**–**d**) and satellite observations **(e)** for different atmospheric conditions over bright surfaces (albedo = 80%). The model results for the MAX-DOAS observations are expressed as ΔAMFs, which are the differences of the AMFs for the low elevation angles and the AMFs for 90° telescope elevation. The ΔAMFs (and also satellite AMFs) are calculated for three different height profiles (constant between 0 and 200 m, constant between 0 and 1000 m, O_4 profile) and for different aerosol profiles (altitude range and total optical density indicated in the figures). Our results indicate that for clear skies the sensitivity of MAX-DOAS observations is about one order of magnitude larger than that of satellite observations. If aerosols are present, the sensitivity for surface-near BrO is substantially reduced (except for the case that the aerosol layer does not reach the ground, see part (d). For satellite observations over high ground albedo, even in the case of high aerosol optical density, the sensitivity for surface near trace gases is still clearly above zero.

ACPD

7, 1823–1847, 2007

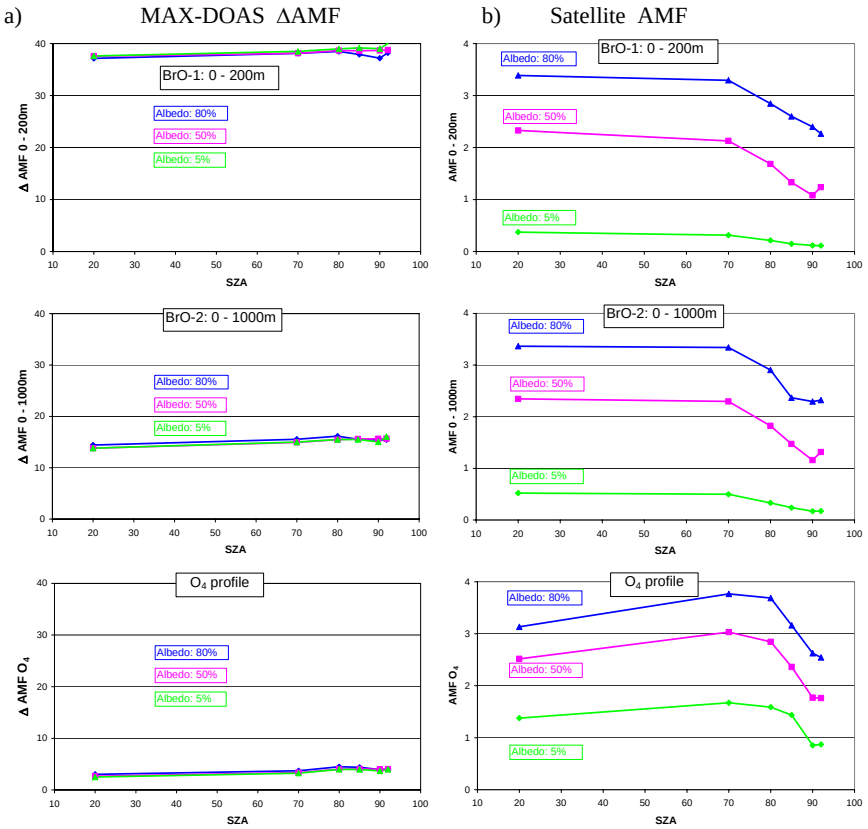

Fig. 2. ΔAMFs for MAX-DOAS observations at 1° elevation angle (left) and AMFs for satellite observations (right) for various values of the surface albedo and different height profiles (see Fig. 1). While the sensitivity of the satellite observations strongly depends on the surface albedo and the solar zenith angle, the ΔAMFs for the MAX-DOAS observations are almost not affected. For the surface near profile the sensitivity of the MAX-DOAS observations is about one order of magnitude larger compared to the satellite observations.

ACPD
7, 1823–1847, 2007

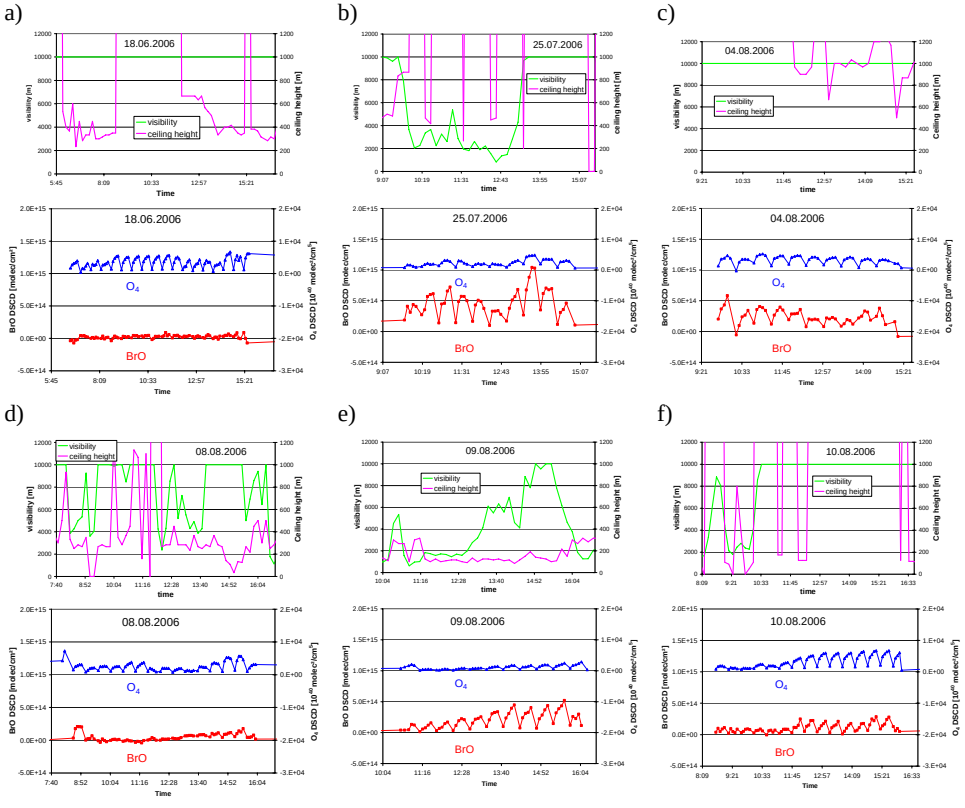

Fig. 3. Measured ΔSCDs of O_4 and BrO for selected days during the ship cruise. Also shown are the horizontal visibility and the ceiling height derived from the on board instrumentation. For cloud ceilings above about 1km, the O_4 absorption is mainly limited by the atmospheric visibility (for an elevation angle of 1° the light path between the telescope and the cloud base is 1 km/sin(1°) ≈57 km). For lower clouds the ceiling height itself becomes also important. High BrO ΔSCDs are observed for almost all observations when the ship was inside the area of first year sea ice (part b to f, for details see text).

ACPD
7, 1823–1847, 2007

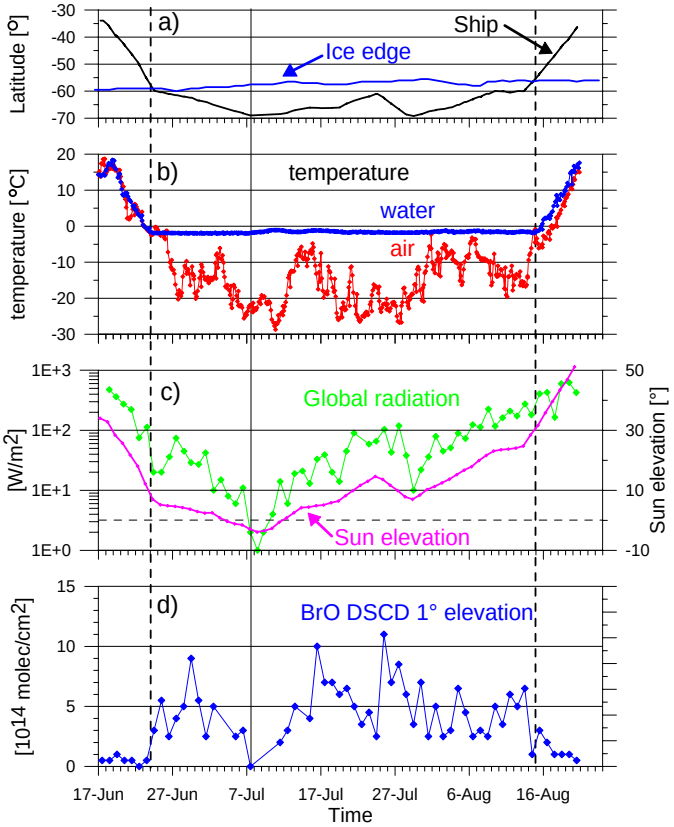

Fig. 4. Daily maximum BrO ΔSCDs for 1° elevation angle **(d)**. Also shown are the latitude of the ship and the ice edge **(a)**, the temperatures of air and water **(b)** as well as daily maximum values of the global radiation and the sun elevation **(c)**. High BrO ΔSCDs are only found for measurements within the area of first year sea ice (indicated also by the water temperature <0°C). For low sun elevation (<–2.8°) also no enhanced BrO ΔSCDs were found.

ACPD
7, 1823–1847, 2007

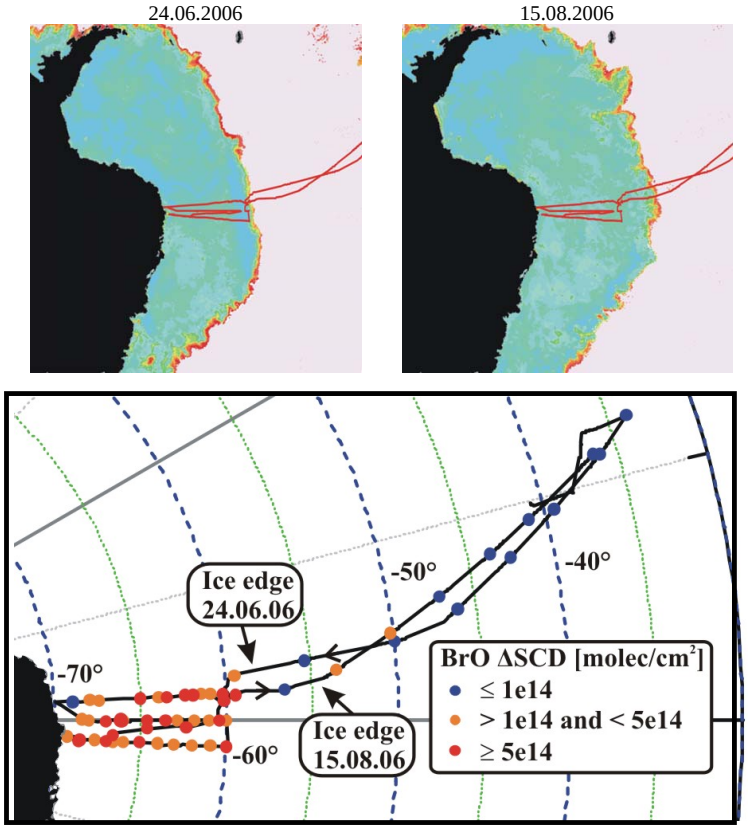

Fig. 5. Top: area of first year sea ice for 24 June 2006 and 15 August 2006 (sea ice data are from the web page of the sea ice group of the National Centers for Environmental Prediction (NCEP) and the Marine Modelling and Analysis Branch (MMAB) (http://polar.ncep.noaa.gov/seaice/). Between these dates the ship was inside the area of first year sea ice. Bottom: daily maximum BrO ΔSCDs for 1° elevation angle. High values are almost exclusively found for measurements within the area of first year sea ice.

ACPD
7, 1823–1847, 2007